Damaged peroxisomes are subject to rapid autophagic degradation in the yeast Hansenula polymorpha

van Zutphen, Tim; Veenhuis, Marten; van der Klei, Ida J.

Published in:
Autophagy

DOI:
10.4161/auto.7.8.15697

BASIC RESEARCH PAPER

Autophagy 7:8, 863-872; August 2011; © 2011 Landes Bioscience

Damaged peroxisomes are subject to rapid autophagic degradation in the yeast *Hansenula polymorpha*

Tim van Zutphen, Marten Veenhuis and Ida J. van der Klei*

Molecular Cell Biology; Groningen Biomolecular Sciences and Biotechnology Institute; Kluyver Centre for Genomics of Industrial Fermentation; University of Groningen; Groningen, The Netherlands

Key words: Pex3, degron, pexophagy, autophagy, *Hansenula polymorpha*

Evidence is accumulating that damaged components of eukaryotic cells are removed by autophagic degradation (e.g., mitophagy). Here we show that peroxisomes that are damaged by the abrupt removal of the membrane protein Pex3 are massively and rapidly degraded even when the cells are placed at peroxisome-inducing conditions and hence need the organelles for growth. Pex3 degradation was induced by a temperature shift using *Hansenula polymorpha pex3*Δ cells producing a Pex3 fusion protein containing an N-terminal temperature sensitive degron sequence. The massive peroxisome degradation process, associated with Pex3 degradation, showed properties of both micro- and macropexophagy and was dependent on Atg1 and Ypt7. This mode of peroxisome degradation is of physiological significance as it was also observed at conditions that excessive ROS is formed from peroxisome metabolism, i.e., when methanol-grown wild-type cells are exposed to methanol excess conditions.

Introduction

Autophagy is a catabolic process of eukaryotic cells that serves to degrade and recycle cytoplasmic components. This is not only required for survival during nutrient starvation, but also important for cellular housekeeping as it removes exhausted, redundant or unwanted components, also including whole, or parts of, organelles. The latter is, for instance, observed for dysfunctional mitochondria.[1,2] In this way autophagy may act as a quality control mechanism preventing cell deterioration or supporting cell remodeling during development. The importance of autophagy in human health and disease is underscored by the finding that autophagy malfunction is linked to several serious diseases such as cancer, neurodegenerative diseases and lysosomal storage diseases.[3,4]

Methylotrophic yeast species (i.e., *Hansenula polymorpha* and *Pichia pastoris*) are attractive models to study the principles of peroxisome autophagy (also designated pexophagy), as in these organisms peroxisome turnover can be precisely prescribed by placing the cells in conditions in which the organelles are redundant for growth.[5,6] As yet, two modes of autophagic peroxisome degradation have been documented, namely micro- and macropexophagy.[7] In *P. pastoris* degradation of peroxisomes by micropexophagy is observed upon a shift of cells from methanol to glucose-containing media. In these conditions, clusters of peroxisomes are taken up by the vacuole for degradation and recycling.[8] In *H. polymorpha* macropexophagy is induced upon shifting cells from methanol to glucose or ethanol media.[9] During glucose-induced macropexophagy the organelles are characteristically sequentially degraded. In particular, large, mature organelles are degraded whereas at least one relatively small organelle escapes this process.[10] In addition to *ATG* genes that encode components of the general autophagy machinery, specific proteins are also required for pexophagy.[11]

We previously identified two peroxisomal membrane proteins (Pex14 and Pex3) that are crucial for both peroxisome biogenesis and autophagy.[12,13] Recently *P. pastoris* Atg30, a peroxisomal membrane protein,[14] as well as *S. cerevisiae* Slt2p, a mitogen-activated protein kinase (MAPK),[15] have been identified to play a role in pexophagy, but not in other selective or nonselective autophagy processes. Interestingly, Atg30 physically interacts with Pex14 and Pex3. In mammals, ubiquination of specific membrane proteins may also initiate their autophagic degradation.[16]

In wild-type *H. polymorpha*, peroxisomes are shown to have a limited life span. During normal vegetative reproduction of cells Atg1-dependent constitutive peroxisome degradation has been observed.[17] Constitutive degradation may possibly be physiologically significant for continuous rejuvenating the peroxisome population by removing exhausted or dysfunctional organelles. As dysfunction of yeast peroxisomes may result in necrotic cell death, timely recognition and turnover of such organelles is of crucial importance, thus stressing the significance of autophagy in cell vitality.[18]

*Correspondence to: Ida J. van der Klei; Email: I.J.van.der.klei@rug.nl
Submitted: 07/16/10; Revised: 03/17/11; Accepted: 04/03/11
DOI: 10.4161/auto.7.8.15697

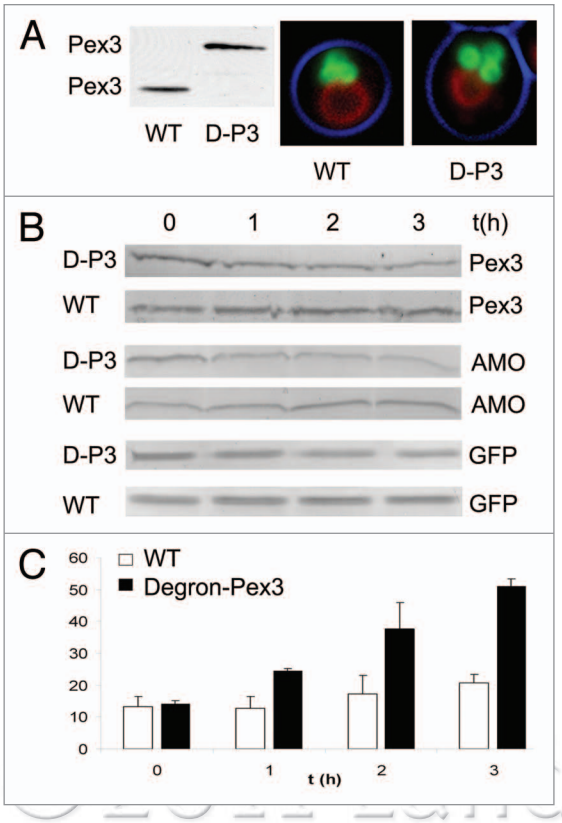

Figure 1. Conditional Pex3 degradation induces peroxisome degradation. (A) Left: Western blot analysis of WT and degron-Pex3^{ts} cells cultured at 25°C on methanol/methylamine containing medium, showing the protein level of Pex3 or Arg-DHFR^{ts}-Pex3 (D-P3). Right: Merged fluorescence microscopy images of WT and degron-Pex3^{ts} (D-P3) cells expressing P_{AMO}-driven *GFP-SKL* cultured at 25°C on methanol/methylamine. Cells contain multiple peroxisomes (green fluorescence); vacuoles are marked red by FM4-64. The cell contours are indicated in blue. (B) Western blot analysis of Pex3, amine oxidase (AMO) and GFP levels in the above WT and degron-Pex3^{ts} cells. Cells were pre-grown at 25°C on methanol/methylamine medium, subsequently supplemented with excess ammonium sulphate and after incubation for 30 min. shifted to 37°C to induce Pex3 degradation (T = 0). Samples were taken at regular time intervals after the shift. In the degron-Pex3^{ts} cells Pex3 levels decreased rapidly. In contrast, in WT controls Pex3 levels slightly increased. GFP-SKL and AMO levels in degron-Pex3^{ts} cells also decreased, but not in WT cells. Blots are decorated with the indicated antibodies. D-P3: degron-Pex3^{ts} cells. Equal volumes of culture were loaded per lane. (C) Quantification of cells containing vacuolar GFP before and after the shift of cells to 37°C as detailed in (B). Vacuolar GFP was quantified in Z-stacks at different time-points after the temperature shift. Degron-Pex3^{ts} and WT cells synthesizing GFP-SKL stained with FM4-64 to mark vacuoles were used. Three independent cultures were measured per strain. Over 100 cells were counted per sample, the bars represent the standard deviation.

For different organelles (e.g., mitochondria and peroxisomes), it has been demonstrated that one or more proteins exposed at the surface of these organelles are essential for their turnover, suggesting that the signal for degradation may originate from the target organelle itself.[12,14,19-22]

To elucidate if induced damage to the peroxisomes leads to their turnover, we investigated the fate of the organelles after removal of Pex3 from the membrane at nutrient excess conditions, using a Pex3 protein fused to a temperature-sensitive degron. The data show that at restrictive temperatures, peroxisome degradation is rapidly induced by a fast degradation mechanism. This mode of organelle degradation was also observed in wild-type cells, when methanol grown cells were exposed to excess methanol conditions.

Results

Conditional degradation of Pex3 results in peroxisome autophagy. To address whether peroxisome damage induced by artificial degradation of Pex3 at peroxisome-inducing cultivation conditions results in organelle degradation, we took advantage of a temperature-sensitive (ts) degron, which consists of a ts-DHFR variant containing an N-terminal Arg (Arg-DHFR^{ts}).[23] *ARG-DHFR^{ts}* was fused to full-length *PEX3* and introduced in *H. polymorpha pex3*Δ cells. During growth of this strain at permissive temperatures (25°C) the cells contained normal peroxisomes and Pex3 levels were akin to WT cells (**Fig. 1A**). We analyzed the fate of peroxisomes upon shifting cells of the degron-Pex3^{ts} strain from the permissive to the restrictive temperature. In order to allow specific analysis of the organelle population present prior to the shift, we introduced the peroxisomal matrix marker *GFP-SKL* under the control of the substrate-inducible amine oxidase promoter (P_{AMO}).[24] During cultivation of such cells on methanol/methylamine media, GFP-SKL is synthesized and accumulates in peroxisomes. As shown before, supplementation of these cultures with excess ammonium sulphate fully represses P_{AMO} and thus GFP-SKL synthesis, allowing discrimination between the organelles present prior to the shift and those subsequently formed after prolonged cultivation at methanol/ammonium sulphate conditions.[25]

Degron-Pex3^{ts} cells were pre-grown on methanol/methylamine at 25°C, subsequently supplemented with excess ammonium sulphate, and further incubated for 30 min at 25°C to deplete *AMO* and *GFP-SKL* mRNAs and then shifted to 37°C.[25] Biochemical analysis showed that in the first hours after the shift to 37°C, Pex3 levels strongly decreased (**Fig. 1B**) in conjunction with a decrease in amine oxidase (AMO) and GFP-SKL protein, whereas in WT controls Pex3, GFP-SKL as well as AMO did not decrease, as expected (**Fig. 1B**). Quantification of Pex3 levels from three individual experiments showed a reduction to approximately 60% of the original level 2 h after the shift and to approximately 50% at 4 h (standard deviation 9.0, 10.4 respectively) and reached ±10% 8 h after the shift. These data suggest that peroxisomes are subject to degradation in Degron-Pex3^{ts} cells at peroxisome-inducing conditions. This was confirmed by fluorescence microscopy analysis which revealed that in these cells increasing numbers of vacuoles, the actual sites of peroxisome degradation, were characterized by the presence of GFP fluorescence (**Fig. 1C**). The relatively low numbers of fluorescent vacuoles in WT were expected, since peroxisomes are subject to slow but continuous constitutive degradation during vegetative reproduction of cells.[17]

Pex3 degradation-induced peroxisome turnover is an *ATG1* dependent process. To determine whether the observed peroxisome degradation is an autophagic process, *ATG1* was deleted in the degron-Pex3^{ts} strain that also produces GFP-SKL. These cells

were cultivated at 25°C on methanol/methylamine to induce GFP-SKL synthesis, followed by repression of GFP-SKL synthesis by excess ammonium sulphate and a subsequent shift of the culture to 37°C. Western blot analysis indicated that the GFP-SKL and amine oxidase (AMO) protein levels remained constant in this strain after the shift (**Fig. 2A**). Moreover, vacuolar GFP was never observed (data not shown), consistent with the view that peroxisome degradation in *atg1*Δ degron-Pex3^{ts} is inhibited and thus represents an autophagic process. As expected, the levels of Pex3 progressively reduced in these cells (**Fig. 2A**).

Pex3 degradation-induced peroxisome turnover is inhibited by CHX. We previously reported that in *H. polymorpha* N-starvation-induced microautophagy, but not glucose-induced macropexophagy, is dependent on protein synthesis. To study whether peroxisome degradation induced in the degron-Pex3^{ts} strain upon a temperature shift is dependent on protein synthesis, we repeated the degradation experiments in the presence of cycloheximide (CHX).[26] The data, presented in **Figure 2B**, show that peroxisome degradation is inhibited in the presence of CHX, suggesting that the process may display characteristics of microautophagy.

Pex3 degradation-induced peroxisome autophagy is selective. To analyze whether the induced degradation process is selective for peroxisomes, we also determined the fate of the cytosolic proteins alcohol dehydrogenase (ADH) and Hsp70, as well as of mitochondrial malate dehydrogenase (MDH). The levels of ADH, Hsp70 and MDH, however, did not decrease upon shifting cells to nonpermissive temperature (**Fig. 2C**), consistent with the view that the Pex3-degradation induced autophagy process is selective for peroxisomes. In addition Hsp70 also increased in a similar manner as ADH and MDH, suggesting no heat shock response was induced by the conditions used, in agreement with the thermotolerant nature of *H. polymorpha*.[27]

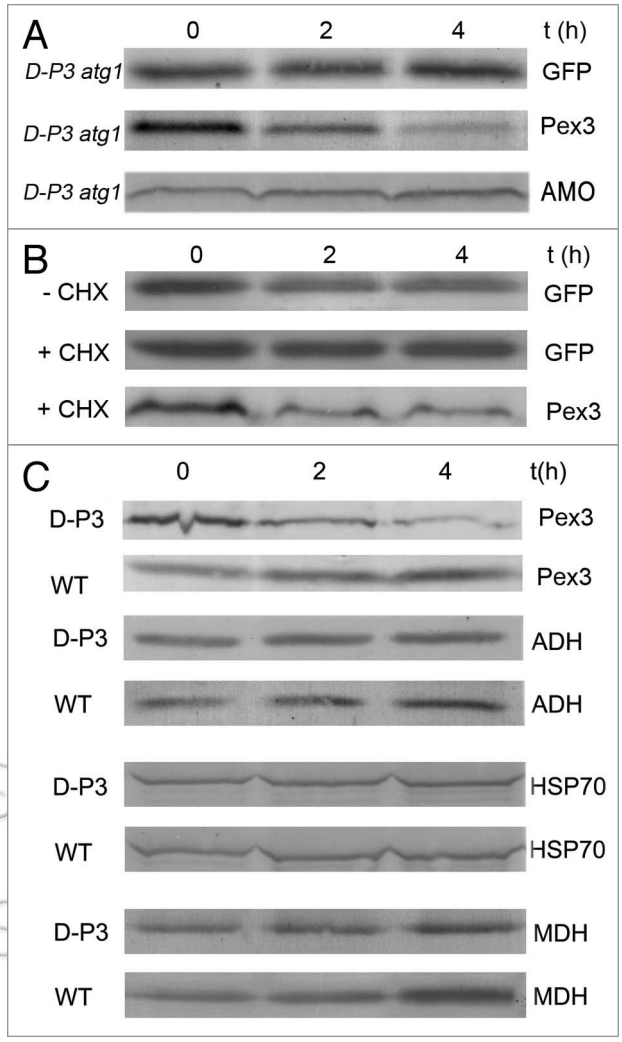

Figure 2. Pex3 degradation-induced peroxisome degradation is an autophagic process. (A) Deletion of *ATG1* in degron-Pex3^{ts} expressing P_{AMO} driven *GFP-SKL* abolished the decrease of GFP-SKL after the shift to 37°C (cultured as described for Fig. 1B). Pex3 levels decreased, similar to the decrease observed for degron-Pex3^{ts} cells. (B) Addition of 6 mg/ml cycloheximide (CHX) also inhibited the degradation of GFP-SKL, but not of Pex3. Cells were cultivated as described at **Figure 1B**. (C) The levels of cytosolic heat shock protein 70 (Hsp70) and alcohol dehydrogenase (ADH) as well as the mitochondrial malate dehydrogenase (MDH) increased in time after the shift to 37°C, whereas Pex3 levels declined rapidly, indicating that the degradation process is specific for peroxisomes. WT and the degron-Pex3^{ts} strains producing GFP-SKL were cultivated as described at Figure 1B. Equal volumes of culture were loaded per lane.

Morphological characteristics of Pex3 degradation-induced pexophagy. The finding that degron-Pex3 induced peroxisome degradation shares properties with N-starvation induced microautophagy and glucose-induced selective macropexophagy, led us to investigate the morphological events of this process by fluorescence and electron microscopy. Fluorescence microscopy analysis revealed that cells, grown on methanol to the mid-exponential growth phase, contained multiple peroxisomes (**Figs. 3A and 4A**). Upon the temperature shift, the degradation process initiated with the formation of an extension of the vacuole directed towards peroxisomes (**Fig. 3B**). Subsequently, a weak FM4-64 fluorescent ring was observed surrounding the organelle (**Fig. 3C**). These rings were invariably completely surrounding the organelles. Next peroxisomes were degraded as judged from the appearance of GFP fluorescence in the vacuole (**Fig. 3D**). At a later stage of cultivation, 2 h after the shift to 37°C, the bulk of the cells contained a single enlarged peroxisome (**Fig. 3E**), whereas identically grown WT control cells contained several peroxisomes (**Fig. 3F**). We never observed bulk uptake of peroxisomes into the vacuole in WT cells, characteristic for macropexophagy.

The ultrastructural details of the degradation process were further examined by electron microscopy. Prior to the shift the degron-Pex3^{ts} cells contained multiple peroxisomes (**Fig. 4A**) per cell. Electron microscopy analysis confirmed the formation of vacuole elongations towards peroxisomes (**Fig. 4B**). Invariably, prior to degradation, electron-dense membrane layers were observed of varying length, positioned in between the peroxisome and the vacuole extension at the site of vacuole-peroxisome tethering (**Fig. 4B and C**). These membranes adhered to the organelle comparable as in macropexophagy (**Fig. 4D**).[5]

In a next stage the peroxisomes appeared less electron dense and subsequently the vacuole is observed invading one or multiple

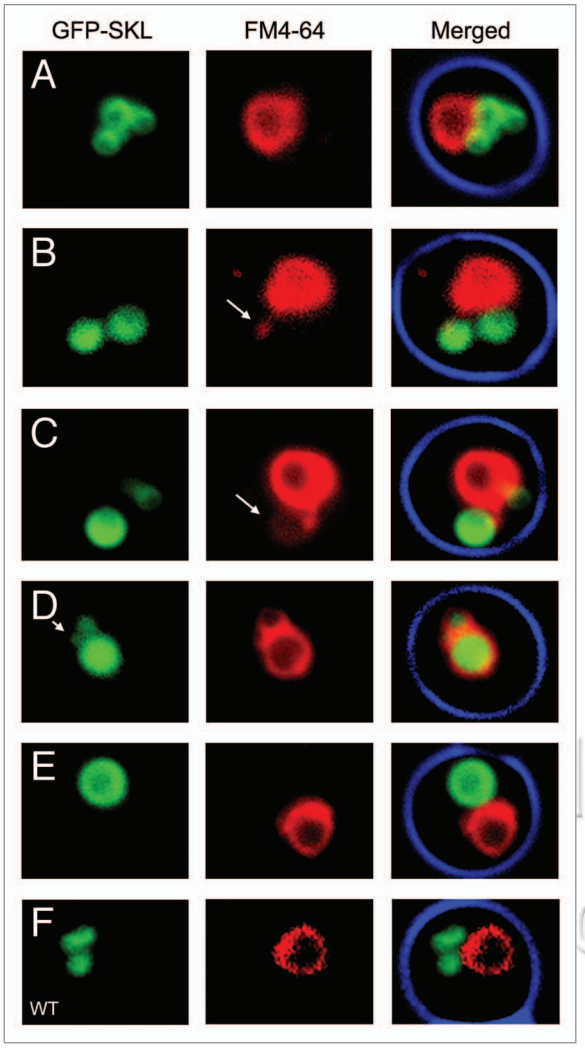

Figure 3. Fluorescence microscopy of Pex3 degradation-induced peroxisome degradation. Fluorescence microscopy of degron-Pex3^{ts} cells expressing P_{AMO}-driven *GFP-SKL* shifted from 25°C to 37°C and grown as described at Figure 1B. (A) Prior to the shift rounded vacuoles marked by FM4-64 and multiple peroxisomes are observed. (B) Thirty min after the shift vacuolar elongations were observed (arrow), superimposed on a peroxisome (T = 30 min.). (C) Subsequently a faint red fluorescent ring (arrow) became visible surrounding a peroxisome (T = 45 min.). (D) Next vacuoles containing diffuse GFP signal were observed (T = 1.5 h), note the small organelle next to the vacuole (arrow). (E) After 2 h most cells contained a single enlarged peroxisome and a round vacuole, whereas WT cells shifted to 37°C for 2 h still contained multiple peroxisomes (F).

organelles (**Fig. 4E and F**), followed by degradation of the organelle (**Fig. 4G**).

Remarkably, normal vacuoles were observed adjacent to organelles that were subject to degradation. The degrading organelles were characterized by the presence of alcohol oxidase protein, judged from immunocytochemistry (**Fig. 4G**). After 2 to 3 h of cultivation at restrictive temperature, bulk of the cells was observed containing a single enlarged peroxisome (**Fig. 4H**).

Atg8-containing membranes are formed during Pex3-degradation-induced pexophagy. To further analyze whether the observed electron-dense membrane structures at the site of vacuole-peroxisome tethering relate to autophagosomes, we analyzed the fate of Atg8 in this process. To this end we introduced BFP-SKL to mark peroxisomes together with GFP-ATG8 in the degron-Pex3^{ts} strain. When these cells were grown on methanol/methylamine at 25°C, bulk of the cells contained cytosolic GFP-Atg8 in conjunction with GFP fluorescence in the vacuole lumen (**Fig. 5A**). This vacuolar GFP fluorescence is most likely related to general autophagy and the relative stability of GFP, which was indicated by the finding that vacuoles also displayed fluorescence when the cells were shifted to other carbon sources, i.e., ethanol instead of methanol at 25°C (data not shown).[28,29] In addition, GFP-Atg8 is frequently seen as a spot, adjacent to the vacuole, which probably represents the phagophore assembly site (PAS; **Fig. 5A**).[30] The typical vacuole extension characteristic at the initial step of organelle turnover was associated with the presence of GFP-Atg8 fluorescence (**Fig. 5B and C**). In the next step a GFP-Atg8 fluorescent ring is observed surrounding the organelle, characterized by the presence of BFP-SKL, whereas the vacuole extension was still observed in close proximity of a peroxisome (**Fig. 5D**). Subsequently, the organelle is encompassed by a weak GFP-Atg8 fluorescent ring that also showed FM4-64 fluorescence (**Fig. 5E**). After fusion with a vacuolar vesicle (compare also **Fig. 4G**) the organelle content is degraded (**Fig. 5F and G**).

The degradation process is dependent on Ypt7. To analyze the requirements of the possible membrane fusion events in the peroxisome degradation process, we analyzed the effect of deleting *YPT7* in the degron-Pex3^{ts} strain producing BFP-SKL and GFP-ATG8. Ypt7 is known to mediate homotypic vacuole fusion and fusion of vacuoles with autophagosomes.[31,32] Cells grown on methanol/methylamine showed vacuole fragmentation, typical for *ypt7*Δ cells and GFP-Atg8 fluorescence located in the cytosol. Upon a shift of such cells from permissive to restrictive temperatures, we failed to detect any GFP-Atg8 and/or FM4-64 fluorescent rings surrounding individual peroxisomes and peroxisome degradation was never observed (**Fig. 6A**). This was confirmed by electron microscopy analysis, which showed that the electron-dense membranes were normally formed (**Fig. 6B**), but degradation of peroxisomes was not observed (not shown).

These data led us to conclude that the Pex3 degradation-induced peroxisome turnover is dependent on Ypt7.

Rapid peroxisome degradation can also be induced in WT cells. We finally addressed whether the conditional mechanism of peroxisome degradation is of physiological significance and also occurs in *H. polymorpha* WT cells. To this end, we chose conditions that result in inactivation of the matrix enzyme alcohol oxidase, namely exposure of methanol-grown cells to excess methanol conditions.[33] At these conditions enhanced levels of formaldehyde and hydrogen peroxide are formed.[33] Addition of 1% methanol to *H. polymorpha* WT cells that were in the late-exponential growth phase on methanol resulted in a growth arrest of approximately 2 h and a transient increase in formation of reactive oxygen species (ROS; **Fig. 7A**). During this phase we also observed degradation of the peroxisomal marker proteins AO, Pex3 and Pex14 (**Fig. 7B**). Morphologically, the process displayed the same structural characteristics as the conditional

Pex3 degradation-induced pexophagy (**Fig. 7C and D**). Similar observations were made during re-examination of cold shock induced peroxisome degradation (not shown).[34] From these experiments we conclude that the above mechanism of peroxisome degradation is a physiological important mechanism for rapidly adjusting peroxisome populations to prevailing environmental conditions.

Discussion

In this study we present evidence that in *Hansenula polymorpha* damaging of peroxisomes by conditional degradation of Pex3 at peroxisome-inducing growth conditions is associated with the rapid, selective autophagic turnover of the organelles. This suggests that Pex3 is an important component in peroxisome maintenance and consistent with the current view that the trigger of organelle turnover may be in the organelle membrane itself.[12-14,19,20,35]

A similar peroxisome degradation process was observed in wild-type cells, upon exposure to methanol-excess conditions and during cold shock induced pexophagy.

During this degradation process features of both microautophagy and macropexophagy were observed. As for microautophagy, the process is dependent on protein synthesis and multiple organelles can be subject to degradation at the same time.[26] However, the morphological events of the degradation process also share distinct characteristics of macropexophagy. The electron-dense membranes that are first formed resemble autophagosomal membranes as in macropexophagy. Also, these membranes contain Atg8, like autophagosomal membranes, supporting that the degradation resembles macroautophagy. The electron-dense membrane may also represent a MIPA-like structure, an Atg8-containing membrane vesicle that is involved in the sequestration of peroxisomes during micropexophagy in *P. pastoris*.[36,37]

The principles of the Pex3 degradation-induced pexophagy process are not yet clear. One option is that the Pex3 degradation-induced process is indeed macropexophagy. However, multiple peroxisomes may be subject to degradation at the same time which has never been observed in

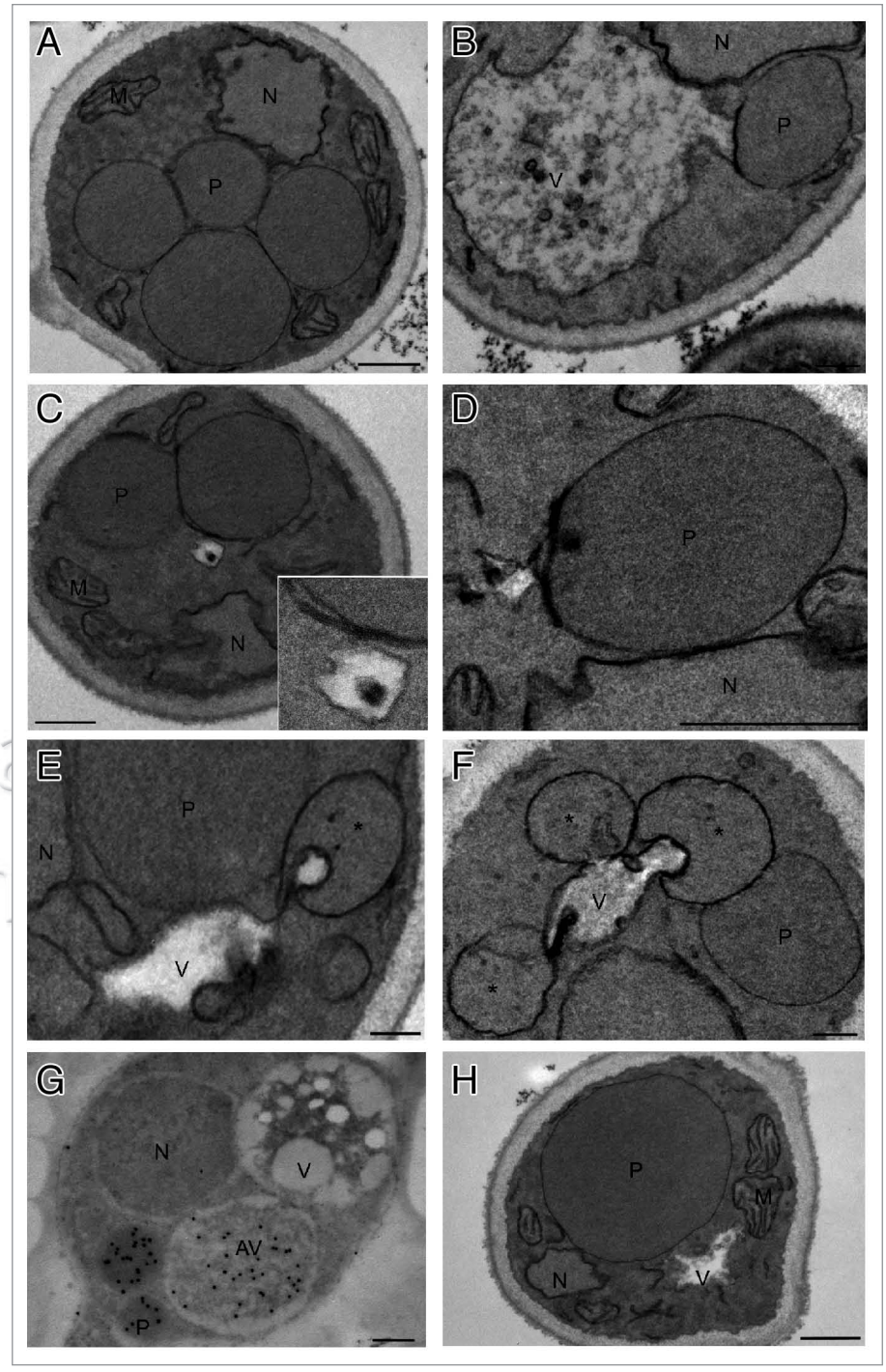

Figure 4. Electron microscopy of Pex3 degradation-induced pexophagy. Ultrathin sections of $KMnO_4$-fixed degron-Pex3^{ts} cells, grown on methanol at 25°C, showing the presence of multiple peroxisomes (A). (B) 30 min after the shift from 25°C to 37°C vacuolar elongations were observed in close proximity to a peroxisome. (C) Invariably electron-dense membrane structures were observed in between the vacuole and peroxisome (enlarged in inset, T = 30 min.). (D) These membranes adhered to the peroxisomal membrane, which was accompanied by decreased electron density of the matrix. Also, (E) invasion of the vacuole extension into one organelle or multiple peroxisomes was observed (T = 1 h). (F) Note the decrease in electron density of these organelles (asterisk). (G) Autophagic vacuoles (AV) contained alcohol oxidase protein evident from immunocytochemistry, using anti-alcohol oxidase antibodies, and were present in conjunction with normal vacuoles that were not labeled for AO protein (T = 2 h). (H) After 2–3 h of incubation bulk of the cells contained a single enlarged peroxisome (T = 2 h). AV-autophagic vacuole, M-mitochondrion, N-nucleus, P-peroxisome, V-vacuole. The bar represents 0.2 μm, except in (A and H): 0.5 μm.

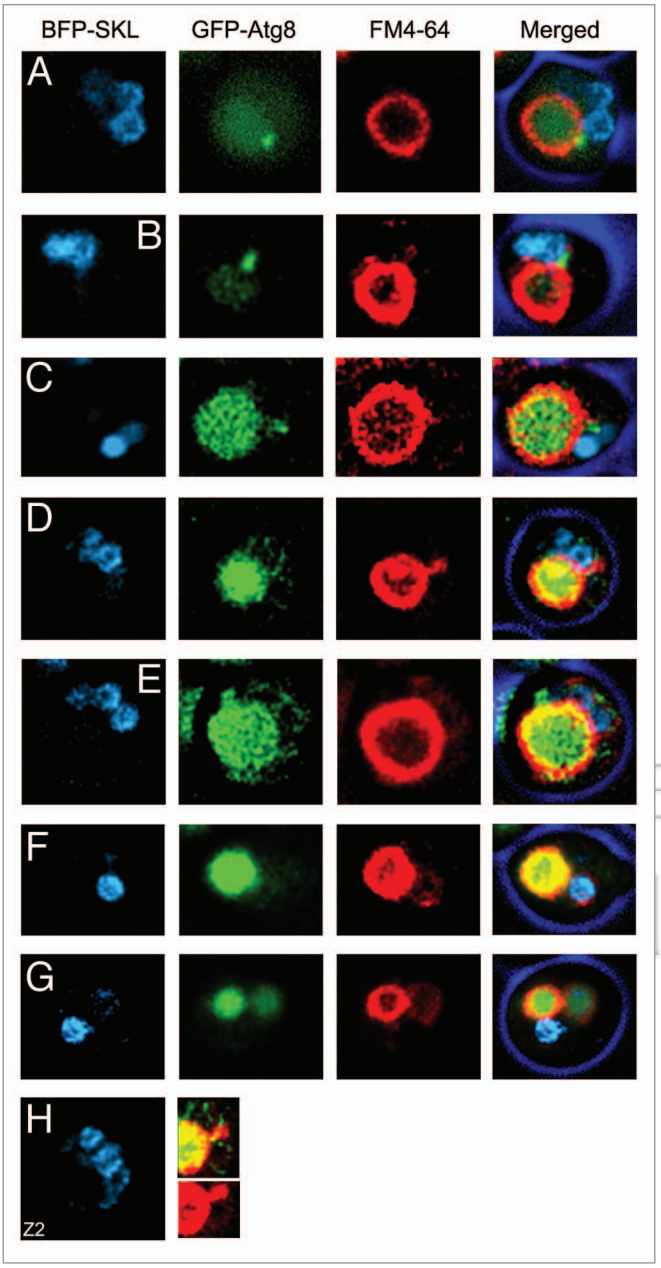

Figure 5. Atg8 localizes to the site of peroxisome degradation. Prior to the shift to restrictive temperature of methanol/methylamine-grown degron-Pex3^{ts} cells expressing *BFP-SKL* and *GFP-ATG8*, GFP-Atg8 localized to the cytosol as well as to the vacuole. Cells characteristically contain a large, round vacuole (red, marked by FM4-64) and multiple peroxisomes (blue, labeled with BFP-SKL). (A) Shortly after the temperature shift (T = 15 min.) also a perivacuolar spot appeared in many cells. (B) Upon formation of the vacuolar extension, GFP-Atg8 was enriched at this structure, which was observed first in close proximity of a peroxisome (T= 15 min). (C) Next GFP-Atg8 extended farther from the vacuole and co-localized with the periphery of the organelle (T = 30 min), resulting in the formation of a GFP-fluorescent ring around a peroxisome (T = 30 min) and a GFP- and FM4-64-double-stained ring (T = 30 min) (E). Often multiple organelles were affected simultaneously. Note the GFP-stained ring above the extension in (D) and the GFP-FM4-64-double-stained ring below the extension (details depicted with higher intensity in "H"), which is surrounding a peroxisome positioned somewhat deeper in the cell (H: BFP-SKL of the next layer of the Z-stack 0.35 μm deeper). Also in (E) multiple peroxisomes are targeted. (F) The GFP-fluorescent ring was no longer observed shortly after formation of the autophagic vacuole (T = 1 h), while also the peroxisome appeared disintegrated (T = 1.5 h) (G). Cells were cultivated until mid-exponential growth phase on methanol/ammonium sulphate, followed by a shift to methanol/methylamine for 14 h (to induce *GFP-ATG8*) and a subsequent shift to 37°C to induce peroxisome degradation.

glucose-induced macropexophagy in *H. polymorpha*. On the other hand, multiple organelle degradation is not unexpected because of the abrupt degradation of Pex3 most likely affects all organelles at the same time upon the shift of cells to nonpermissive temperature. The massive need for sequestering membranes to form pexophagosomes in this case may add to the explanation why the process is dependent of protein synthesis. Consequently, in this case macropexophagy in *H. polymorpha* may affect multiple organelles at the same time in specific conditions. This is confirmed by the observations of rapid peroxisome turnover after exposure of methanol-grown cell to excess methanol or a cold shock.

An alternative explanation may be that the above degradation process represents an adapted type of autophagy, which involves fusion of the electron-dense membranes with the peroxisomal membrane prior to fusion with the vacuole. This fusion process may make the organelle compatible for subsequent fusion with the vacuole membrane and protect the surrounding membrane from degradation by vacuolar hydrolases as it has acquired properties of the electron-dense membrane. This option is however still speculative.

Materials and Methods

Organisms and growth. The *H. polymorpha* strains that were used in this study are listed in **Table 1**. Cultivation was performed using either YPD (1% yeast extract, 1% peptone, 1% glucose) supplemented with appropriate antibiotics or mineral medium containing 0.25% (w/v) ammonium sulphate or methylamine as nitrogen source and 0.5% (w/v) glucose or methanol (v/v) as carbon source, supplemented with 30 mg/l leucine.

Escherichia coli XL1 Blue was grown on LB supplemented with appropriate antibiotics.

Construction of strains. An expression cassette was constructed that encoded a part of mouse dihydrofolate reductase containing an N-terminal arginine (Arg-DHFR^{ts}, degron)[23] fused to the N-terminus of full length Pex3. pHipZ6.*DEGRON-PEX3^{ts}* was constructed as follows; the degron-cassette was amplified from pKL187 (Euroscarf collection) using primer degron-Pex3 Fw CGC GCG GCC GCG CAT GCA GAT TTT CGT CAA GAC and primer degron-Pex3 Rv AGA TCT GGC ACC CGC TCC AGC GCC TGC A. NotI-BglII digested PCR-product was ligated into NotI-BamHI digested pHipX7-*PEX3*.[41] A SphI-SalI fragment *DEGRON-PEX3^{ts}* was ligated into SphI-SalI digested pHipZ6, generating pHipZ6.*DEGRON-PEX3^{ts}*.[42] The linearized vector (BsiWI) was integrated into *H. polymorpha pex3*Δ, resulting in strain degron-Pex3^{ts}. Correct integration was confirmed by Southern blot analysis.[43]

Linearized (BsiWI) pHipX5-e*GFP-SKL* was integrated to label peroxisomes in degron-Pex3^{ts}.[39]

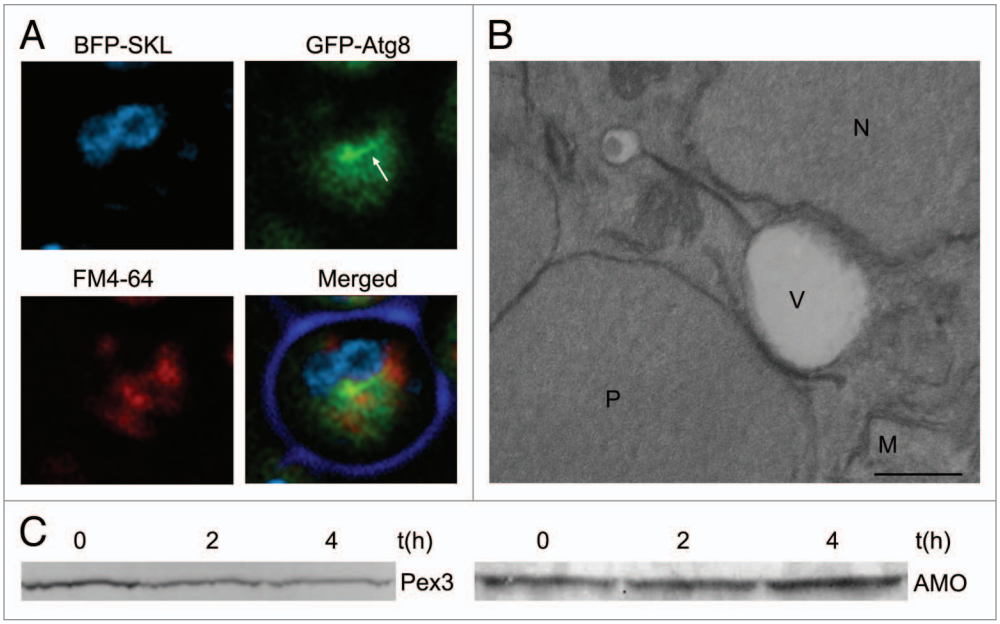

Figure 6. Ypt7 is required for organelle degradation. *Ypt7*Δdegron-Pex3^{ts} cells expressing *BFP-SKL* and *GFP-ATG8* often contained GFP-containing structures in close proximity of peroxisomes after the shift to 37°C and fragmented vacuoles (T = 1) (A), however no GFP- or FM4-64-stained rings were observed at any of the time points these structures were observed in degron-Pex3^{ts} cells. (B) Ultrastructural analysis showed highly fragmented vacuoles and various membrane patches in the cytosol, often close to peroxisomes, resembling the initial stages of Pex3 degradation-induced pexophagy (T = 1, as shown in 4D). No difference in appearance of these organelles could be observed before and after the temperature shift. M-mitochondrion, N-nucleus, P-peroxisome. The bar represents 0.2 μm. (C) Western blot analysis of Pex3 and amine oxidase (AMO) levels in *Ypt7*Δdegron-Pex3^{ts} cells showed that the levels of Pex3, but not of AMO decreased upon a shift to restrictive temperature. Cells grown on methanol/methylamine were supplemented with excess ammonium sulphate for 30 min and shifted to the restrictive temperature. In similarly grown degron-Pex3^{ts} cells both Pex3 and AMO levels decreased after the shift (compare **Fig. 1B**).

*Atg1*Δ degron-Pex3^{ts} was generated by replacing *URA3* by *NAT1* in the original *ATG1* deletion cassette and integration of an ApaI-NdeI fragment in the degron-Pex3^{ts} strain expressing *eGFP-SKL*. PBS-*PDD7-URA* was digested with SalI, self-ligated, followed by digestion with EcoRI-HindIII and ligation of an EcoRI-HindIII fragment from pAG25 containing *NAT1*, generating pBS-*PDD7-NAT1*.[44,45] Integration was confirmed by Southern blot analysis.

For Atg8 localization, *eGFP-ATG8* was isolated from pHipX6-*eGFP-ATG8* by SmaI-BamHI digestion and ligation into pHipN5.[46] Linearized (StuI) pHipX4 *eBFP2-SKL* was integrated into degron-Pex3^{ts}, followed by integration of linearized (Bsu36I) pHipN5-*eGFP-ATG8*.[47]

YPT7 deletion was obtained by replacing the first 394 nucleotides by the *HPH* gene.[45] Primers Ypt7 Fw GAA GAA GCG ACG CCG ATC CAG TTG ATG TG and Ypt7 Rv GAA AGT ACA AAT GGC GGT GG were used to generate a PCR product which was phosphorylated and ligated into EcoRV-HpaI digested Pag32. Primers Hsp26 Fw GGC AAG CTT TAA GGA CAA GGT CAC CAT TG and Hsp26 Rv CCG GGA TCC GTA AAA TGA TGA GGC AAA GG were used to generate a second PCR product. Both vector and PCR product were digested with HindIII-BamHI and ligated. Integration of the *YPT7* deletion construct into degron-Pex3^{ts} expressing *eBFP2-SKL* and *GFP-ATG8* was confirmed by Southern blot analysis.

Microscopy. Vacuoles were labeled for fluorescence microscopy by the addition of 2 μM FM4-64 (Invitrogen, T3166) to the cultures. Upon incubation for at least 4 h, cells were analyzed with a Zeiss Observer Z1, or LSM 510 confocal laser scanning microscope. For wide-field microscopy eBFP2 was visualized using a 380 nm LED and detected with a 435–485 nm bandpass filer (BP). GFP was excited with a 470 nm LED and detected using a 500–550 nm BP filter. FM4-64 was excited with a 555 nm LED and detected using a 570–640 nm filter. For live-cell imaging, cells were transferred to an objective containing 1% agarose, incubated in the appropriate medium and kept at 37°C; 10% LED power was used for sequential imaging.

For confocal microscopy GFP was visualized by excitation with a 488 nm argon laser (Lasos) and detected using a 500–550 nm BP filter. FM4-64 was excited with a 543 nm helium laser (Lasos) and detected using a 565–615 nm BP filter. To enhance details deconvolution was applied using the classic maximum likelihood method and a theoretical point spread function (Huygens professional v3.3, scientific volume imaging). Electron microscopy using ultrathin sections for morphological and immunocytochemical analysis was performed as described in reference 48.

FACS analysis. To determine the presence of reactive oxygen species, cells were incubated with H_2DCFDA (Invitrogen, D399) for 30 min and analyzed by flow cytometry using a 488 nm laser and 500–550 BP filter (FACS Aria II, Becton Dickinson).[18]

Biochemical methods. SDS-polyacrylamide gel electrophoresis and western blot analysis of cell lysates were performed

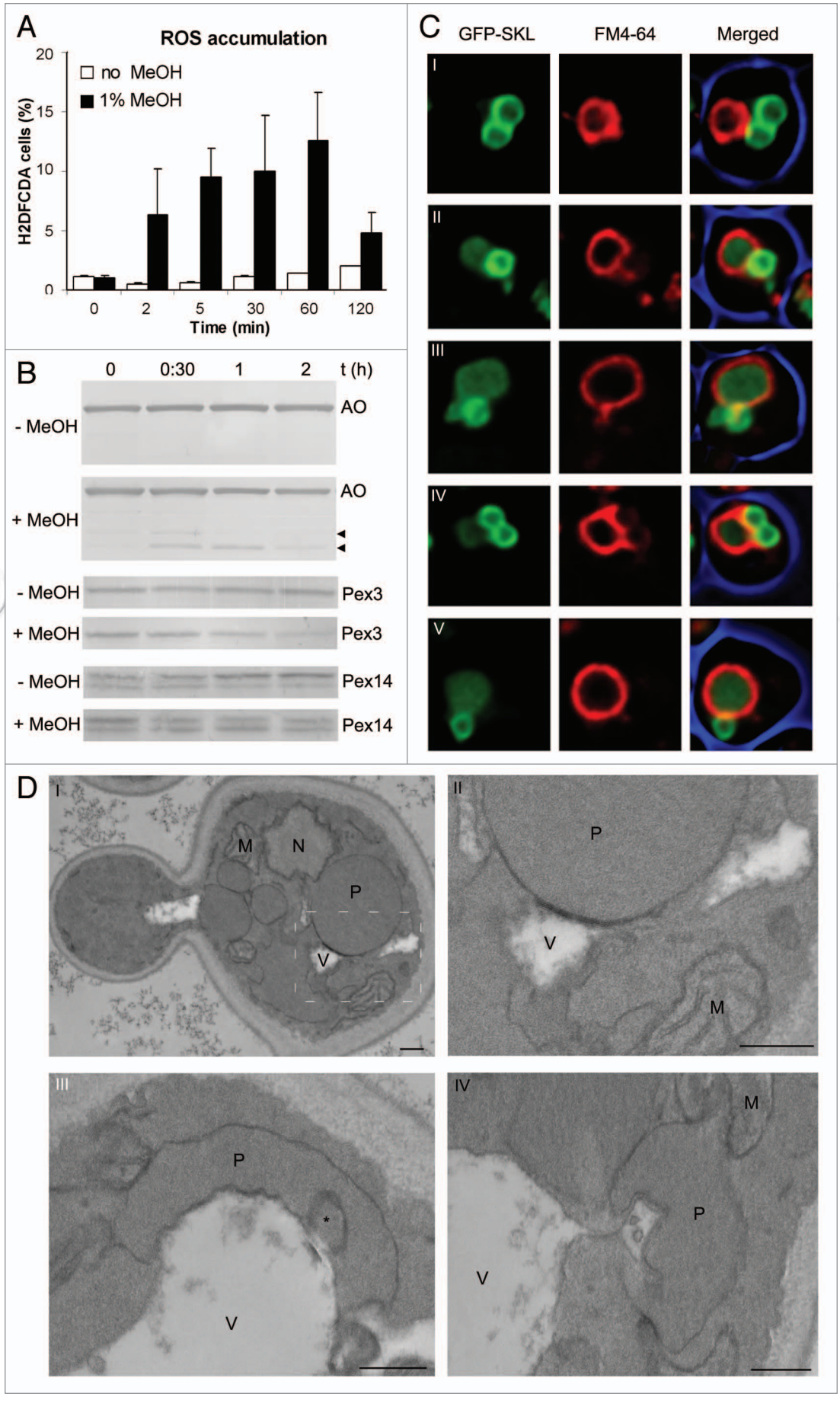
A
ROS accumulation
no MeOH
1% MeOH
H2DFCDA cells (%)
20
15
10
5
0
0
2
5
30
60
120
Time (min)
B
0
0:30
1
2
t (h)
- MeOH
AO
+ MeOH
AO
- MeOH
Pex3
+ MeOH
Pex3
- MeOH
Pex14
+ MeOH
Pex14
C
GFP-SKL
FM4-64
Merged
I
II
III
IV
V
D
I
M
N
P
V
II
P
V
M
III
P
*
V
IV
M
P
V

Figure 7 (See opposite page). Peroxisomes are degraded at methanol excess conditions. Shortly after addition of 1% of methanol to methanol-grown WT cells (OD 1.8), an increase in H_2DFCA-positive cells was observed, indicative for the accumulation of ROS (A). The increase remained approximately constant for 120 min after methanol addition and then decreased. 10,000 cells of three independent cultures were analyzed. The bar represents the standard deviation. (B) Western blot analysis of samples taken at various time-points after methanol addition revealed a decrease in alcohol oxidase (AO) level (degradation products are indicated by arrowheads), indicative of peroxisome degradation. In controls not administrated with excess methanol AO levels were unchanged. Pex3 levels declined rapidly after addition of methanol, while remaining approximately unaffected in controls not supplemented with excess methanol. Pex14 levels showed a pattern reminiscent of glucose-induced macropexophagy; the phosphorylated form (upper band) declined after addition of methanol, while the nonphosphorylated form did not drastically change.[50] In the control the phosphorylated form increased, while the nonphosphorylated form did not change. (C) Prior to addition of methanol, rounded vacuoles and multiple peroxisomes were observed (I), whereas 15 min after addition of 1% methanol, vacuolar extensions appeared in close proximity of peroxisomes (II). These elongations next pointed towards a peroxisome, after which a FM4-64 stained ring appeared around one or even multiple organelles (III, IV, T = 30 min.). One hour after methanol addition most cells contained a single peroxisome and GFP in the central vacuole. (D) Ultrastructural analysis of these cells also showed vacuole vesicles or elongations close to the peroxisomal membrane, with membrane patches in between both organelles (I; enlarged in II, T = 30 min.). Next peroxisomes were observed with invading vacuoles (III; IV, T = 1 h). M-mitochondrion, N-nucleus, P-peroxisome, V-vacuole. Bar represents 0.2 μm.

Table 1. Strains used in this study

Strain	Properties	Reference
WT	Wild-type NCYC 495 *leu1.1*	38
WT. *GFP-SKL*	NCYC 495 *leu 1.1* with pHipX5-*eGFP-SKL* integration (P_{AMO})	39
*pex3*Δ	*PEX3* deletion strain *leu1.1*	40
degron-Pex3^{ts}	*PEX3* deletion strain with double-copy pHipZ6-*DEGRON-PEX3*^{ts} integration *leu 1.1* (P_{PEX3})	This study
degron-Pex3^{ts}. *GFP-SKL*	degron-Pex3^{ts} with pHipX5-*eGFP-SKL* integration (P_{AMO})	This study
*atg1*Δ degron-Pex3^{ts}	*ATG1* deletion in *pex3*Δ::*degron-pex3*. expressing *eGFP-SKL* (P_{AMO})	This study
degron-Pex3^{ts}. *BFP-SKL*. *GFP-ATG8*	*pex3*Δ::*degron-pex3* with pHipX4-e*BFP2-SKL* (P_{aox}) and pHipN5-*eGFP-ATG8* (P_{amo}) integration	This study
*ypt7*Δ degron-Pex3^{ts}	*YPT7* deletion in degron-Pex3^{ts}. BFP-SKL.GFP-ATG8	This study

as detailed previously in reference 49–51. Blots were decorated using rabbit polyclonal antibodies and detected using either the Protoblot immunoblotting system (Promega, W3960) or BM Chemiluminiscence western blotting kit (Roche, 11 520 709 001). Scanning was performed with a densitometer (Biorad GS-710).

Acknowledgements

We thank Ron Booij, Arjen Krikken and Rinse de Boer for skillful assistance in microscopy and Sven Thoms & Ralf Erdmann for kindly providing the degron-cassette. Tim van Zutphen is supported by the Netherlands Organisation for Scientific Research/Earth and Life Sciences (NWO/ALW). This project was carried out within the research program of the Kluyver Centre for Genomics of Industrial Fermentation, which is part of the Netherlands Genomics Initiative/Netherlands Organization for Scientific Research.

References

1. Bhatia-Kiššová I, Camougrand N. Mitophagy in yeast: actors and physiological roles. FEMS Yeast Res 2010; 10:1023-34.
2. Priault M, Salin B, Schaeffer J, Vallette FM, di Rago JP, Martinou JC. Impairing the bioenergetic status and the biogenesis of mitochondria triggers mitophagy in yeast. Cell Death Differ 2005; 12:1613-21.
3. Mizushima N, Levine B, Cuervo AM, Klionsky DJ. Autophagy fights disease through cellular self-digestion. Nature 2008; 451:1069-75.
4. Todde V, Veenhuis M, van der Klei IJ. Autophagy: Principles and significance in health and disease. Biochim Biophys Acta 2009; 1792:3-13.
5. Veenhuis M, Douma A, Harder W, Osumi M. Degradation and turnover of peroxisomes in the yeast *Hansenula polymorpha* induced by selective inactivation of peroxisomal enzymes. Arch Microbiol 1983; 134:193-203.
6. Sakai Y, Oku M, van der Klei IJ, Kiel JAKW. Pexophagy: Autophagic degradation of peroxisomes. Biochim Biophys Acta 2006; 763:1767-75.
7. Tuttle DL, Dunn WA Jr. Divergent modes of autophagy in the methylotrophic yeast *Pichia pastoris*. J Cell Sci 1995; 108:25-35.
8. Sakai Y, Kooler A, Rangell LK, Keller GA, Subramani S. Peroxisome degradation by microautophagy in *Pichia pastoris*: identification of specific steps and morphological intermediates. J Cell Biol 1998; 141:625-36.
9. Veenhuis M, Zwart K, Harder W. Degradation of peroxisomes after transfer of methanol-grown *Hansenula polymorpha* into glucose-containing media. FEMS Microbiol Lett 1978; 3:21-8.
10. Leao-Helder AN, Krikken AM, van der Klei IJ, Kiel JAKW, Veenhuis M. Transcriptional downregulation of peroxisome numbers affects selective peroxisome degradation in *Hansenula polymorpha*. J Biol Chem 2003; 278:40749-56.
11. Meijer WH, van der Kleij IJ, Veenhuis M, Kiel JAKW. *ATG* genes involved in non-selective autophagy are conserved from yeast to man, but the selective CVT and pexophagy pathways also require organism-specific genes. Autophagy 2007; 2:106-16.
12. Veenhuis M, Komori M, Salomons F, Hilbrands RE, Hut H, Baerends RJS, et al. Peroxisome remnants in peroxisome deficient mutants of the yeast *Hansenula polymorpha*. FEBS letters 1996; 383:114-8.
13. Bellu AR, Salomons FA, Kiel JAKW, Veenhuis M, van der Klei IJ. Removal of Pex3p is an important initial stage in selective peroxisome degradation in *Hansenula polymorpha*. J Biol Chem 2002; 277:42875-80.
14. Farre JC, Manjithaya R, Mathewson RD, Subramani S. PpAtg30 tags peroxisomes for turnover by selective autophagy. Dev Cell 2008; 14:365-76.
15. Manjithaya R, Jain S, Farré JC, Subramani S. A yeast MAPK cascade regulates pexophagy but not other autophagy pathways. J Cell Biol 2010; 189:303-10.
16. Kim PK, Hailey DW, Mullen RT, Lippincott-Schwartz J. Ubiquitin signals autophagic degradation of cytosolic proteins and peroxisomes Proc Natl Acad Sci 2008; 105:20567-74.
17. Bener Aksam E, Koek A, Kiel JAKW, Jourdan S, Veenhuis M, van der Klei IJ. A peroxisomal Lon protease and peroxisome degradation by autophagy play key roles in vitality of *Hansenula polymorpha* cells. Autophagy 2007; 3:96-105.
18. Bener Aksam E, Jungwirth H, Kohlwein SD, Ring J, Madeo F, Veenhuis M, et al. Absence of the peroxiredoxin Pmp20 causes peroxisomal protein leakage and necrotic cell death. Free Radic Biol Med 2008; 45:1115-24.
19. Kissova I, Salin B, Schaeffer J, Bhatia S, Manon S, Camougrand N. Selective and non-selective autophagic degradation of mitochondria in yeast. Autophagy 2007; 3:329-36.
20. Kanki T, Wang K, Cao Y, Baba M, Klionsky DJ. Atg32 is a mitochondrial protein that confers selectivity during mitophagy. Dev Cell 2009; 17:98-109.

21. Okamoto K, Kondo-Okamoto N, Ohsumi Y. Mitochondria-anchored receptor Atg32 mediates degradation of mitochondria via selective autiophagy. Dev Cell 2009; 17:87-97.
22. Bellu AR, Komori M, van der Klei IJ, Kiel JAKW, Veenhuis M. Peroxisome biogenesis and selective degradation converge at Pex14p. J Biol Chem 2001; 276:44570-4.
23. Dohmen RJ, WU P, Varshavsky A. Heat-inducible degron: a method for constructing temperature-sensitive mutants. Science 1994; 263:1273-6.
24. Zwart K, Veenhuis M, van Dijken JP, Harder W. Development of amine oxidase-containing peroxisomes in yeasts during growth on glucose in the presence of methylamine as the sole source of nitrogen. Arch Microbiol 1980; 126:117-26.
25. Waterham HR, Titorenko VI, Swaving GJ, Harder W, Veenhuis M. Peroxisomes in the methylotrophic yeast *Hansenula polymorpha* do not necessarily derive from pre-existing organelles. EMBO 1993; 12:4785-94.
26. Monastyrska I, Kiel JAKW, Krikken AM, Komduur JA, Veenhuis M, van der Klei IJ. The *Hansenula polymorpha ATG25* gene enocodes a novel coiled-coil protein that is required for macropexophagy. Autophagy 2005; 1:92-100.
27. Reinders A, Romano I, Wiemken A, de Virgilio C. The thermophilic yeast *Hansenula polymorpha* does not require trehalose synthesis for growth at high temperatures but does for normal acquisition of thermotolerance. J Bacteriol 1999; 181:4665-8.
28. Shintani T, Klionsky DJ. Cargo proteins facilitate the formation of transport vesicles in the cytoplasm to vacuole targeting pathway. J Biol Chem 2004; 279:29889-94.
29. Hara T, Nakamura K, Matsui M, Yamamoto A, Nakahara Y, Suzuki-Migishima R, et al. Supression of basal autophagy in neural cells causes neurodegenerative disease in mice. Nature 2006; 441:885-9.
30. Suzuki K, Kirisako T, Kamada Y, Mizushima N, Noda T, Ohsumi Y. The pre-autophagosomal structure organized by concerted functions of *APG* genes is essential for autophagosome formation. EMBO J 2001; 20:5971-81.
31. Haas A, Scheglmann D, Lazar T, Gallwitz D, Wickner W. The GTPase Ypt7 of *Saccharomyces cerevisiae* is required on both partner vacuoles for the homotypic fusion step of vacuole inheritance. EMBO J 1995; 14:5258-70.
32. Kirisako T, Baba M, Ishihara N, Miyazawa K, Ohsumi M, Yoshimori T, et al. Formation process of autophagosome is traced with Apg8/Aut7p in yeast. J Cell Biol 1999; 147:435-46.
33. Veenhuis M, van Dijken JP, Pilon SAF, Harder W. Development of crystalline peroxisomes in methanol-grown cells of the yeast *Hansenula polymorpha* and its relation to environmental conditions. Arch Microbiol 1978; 117:153-63.
34. Komduur JA, Bellu AR, Knoops K, van der Klei IJ, Veenhuis M. Cold-inducible selective degradation of peroxisomes in *Hansenula polymorpha*. FEMS Yeast Res 2004; 5:281-5.
35. Kiel JAKW, Komduur JA, van der Klei IJ, Veenhuis M. Macropexophagy in *Hansenula polymorpha*: facts and views. FEBS Lett 2003; 549:1-6.
36. Farré JC, Krick R, Subramani S, Thumm M. Turnover of organelles by autophagy in yeast. Curr Opin Cell Biol 2009; 21:522-30.
37. Oku M, Sakai Y. Peroxisomes as dynamic organelles: autophagic degradation. FEBS J 2010; 277:3289-94.
38. Gleeson MAG, Sudbery PE. Genetic analysis in the methylotrophic yeast *Hansenula polymorpha*. Yeast 1988; 4:293-303.
39. Ozimek P, Lahtchev K, Kiel JAKW, Veenhuis M, van der Klei IJ. *Hansenula polymorpha* Swi1p and Snf2p are essential for methanol utilisation. FEMS Yeast Res 2004; 4:673-82.
40. Baerends RJS, Rasmussen SW, Hilbrands RE, van der Heide M, Faber KN, Reuvekamp PT, et al. The *Hansenula polymorpha PER9* gene encodes a peroxisomal membrane protein essential for peroxisome assembly and integrity. J Biol Chem 1996; 271:8887-94.
41. Baerends RJS, Salomons FA, Faber KN, Kiel JAKW, van der Klei IJ, Veenhuis M. Deviant Pex3p levels effect normal peroxisome formation in *Hansenula polymorpha*: high steady-state levels of the protein fully abolish matrix protein import. Yeast 1997; 13:1437-48.
42. Haan GJ, Baerends RJS, Krikken AM, Otzen M, Veenhuis M, van der Klei IJ. Reassembly of peroxisomes in *Hansenula polymorpha* pex3 cells on reintroduction of Pex3p involves the nuclear envelope. FEMS Yeast Res 2006; 6:186-94.
43. Faber KN, Haima P, Harder W, Veenhuis M. Highly-efficient electro-transformation of the yeast *Hansenula polymorpha*. Curr Genet 1994; 25:305-10.
44. Komduur JA, Veenhuis M, Kiel JAKW. The *Hansenula polymorpha PDD7* gene is essential for macropexophagy and microautophagy. FEMS Yeast Res 2003; 3:27-34.
45. Goldstein AL, McCusker JH. Three new dominant drug resistance cassettes for gene disruption in *Saccharomyces cerevisiae*. Yeast 1999; 15:1541-53.
46. Monastyrska I, van der Heide M, Krikken AM, Kiel JAKW, van der Klei IJ, Veenhuis M. Atg8 is essential for Macropexophagy in *Hansenula polymorpha*. Traffic 2005; 6:66-74.
47. Nagotu S, Krikken AM, Otzen M, Kiel JAKW, Veenhuis M, van der Klei IJ. Peroxisome fission in *Hansenula polymorpha* requires Mdv1 and Fis1, two proteins also involved in mitochondrial fission. Traffic 2008; 9:1471-84.
48. Van Zutphen T, van der Klei IJ, Kiel JAKW. Pexophagy in *Hansenula polymorpha*. Methods Enzymol 2008; 451:197-215.
49. Laemmli UK. Cleavage of structural proteins during the assembly of the head of bacteriophage T4. Nature 1970; 227:680-5.
50. Kyhse-Andersen J. Electroblotting of multiple gels: a simple apparatus without buffer tank for rapid transfer of proteins from polyacrylamide to nitrocellulose. Biochem Biophys Methods 1984; 10:203-9.
51. Baerends RJS, Faber KN, Kram AM, Kiel JAKW, van der Klei IJ, Veenhuis M. A stretch of positively charged amino acids at the N terminus of *Hansenula polymorpha* Pex3p is involved in incorporation of the protein into the peroxisomal membrane. J Biol Chem 2000; 275:9986-95.